Photosensitizer-Loaded pH-Responsive Hollow Gold Nanospheres for Single Light-Induced Photothermal/Photodynamic Therapy

ARTICLE *in* ACS APPLIED MATERIALS & INTERFACES · AUGUST 2015

Impact Factor: 6.72 · DOI: 10.1021/acsami.5b05763

5 AUTHORS, INCLUDING:

Meng Yu
Tianjin University
12 PUBLICATIONS **14** CITATIONS
SEE PROFILE

Nan Li
23 PUBLICATIONS **51** CITATIONS
SEE PROFILE

ACS APPLIED MATERIALS & INTERFACES

Letter

www.acsami.org

Photosensitizer-Loaded pH-Responsive Hollow Gold Nanospheres for Single Light-Induced Photothermal/Photodynamic Therapy

Meng Yu,[†] Fang Guo,[†] Jinping Wang,[†] Fengping Tan,*[,†] and Nan Li*[,†]

[†]Tianjin Key Laboratory of Drug Delivery & High-Efficiency, School of Pharmaceutical Science and Technology, Tianjin University, Tianjin 300072, P.R. China

Supporting Information

ABSTRACT: Novel photoinduced triple-response antitumor therapeutic system based on hollow gold nanospheres (HAuNS), pH (low) insertion peptide (pHLIP), and Chlorin e6 (Ce6), was reported for the first time. The system was able to intracellularly deliver the nanocarriers by the transmembrane ability of pHLIP at the condition of pH 6.2. Ce6 and pHLIP were then released from the surface of the carriers due to the weakening electrostatic interaction with HAuNS under the photoirradiation. Herein, HAuNS performed two different functions: (1) as a nanocarrier because of the excellent loading capability; (2) experienced the photothermal therapy (PTT) effect as a photothermal coupling agent (PTCA), thus enhancing the photodynamic therapy (PDT) effect of Ce6.

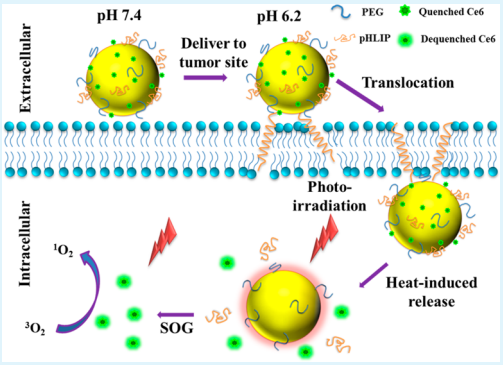

KEYWORDS: *single-light inducement, triple response, one-step PTT/PDT effect, pH-driven targeting, phototriggered release*

The dose of a drug required to achieve clinically effective cytotoxicity in tumors often caused undesirable side effects. Drug-free systems based on PDT were considered to be emerging noninvasive modalities for the treatment of various cancers. Photosensitizer (PS), which is one of the necessary factors of PDT, could absorb light and transfer energy to the oxygen of surrounding tissue. However, the therapeutic efficacy of PDT in solid tumors was limited by the poor water-solubility, as well as inadequate selectivity of most PSs, nonspecific activation in the blood circulation and self-destruction upon photoirradiation.[1,2]

In recent years, new synergistic treatment modalities, which combined with other therapies such as PTT, hold the promise to overcome the current limitations of PDT, thus achieving enhanced anticancer efficacy.[2−4] However, synergistic PDT/PTT efficacy was largely limited by two issues: (1) two lasers in different wavelengths were needed for PDT/PTT because of the absorption mismatch of photothermal coupling agents (PTCAs) and PSs,[3,5] which would result in a relatively higher cost and longer therapeutic time; (2) limited surface area of nanoparticles, which might be due to the relatively lower loading capacity of PSs. To solve the problems, we used hollow gold nanosphere (HAuNS) both as the nanocarrier and PTCA in this study because of its strong and tunable absorption in the vis−NIR region and greater loading surface area.[6,7]

In addition, ROS performed a relatively short lifetime in biological systems (<0.04 μs) and small active region (<0.02 μm),[8] which meant that the targeted delivery of PSs to the tumor cells was very important for the efficient PDT. Recently, Weerakkody et al. had illuminated the fast pH-driven ability of pHLIP family for tumor targeting.[9] Besides, pHLIP has been demonstrated to actively and rapidly insert into the lipid bilayer and translocate its C-terminus into cells upon change of the pH value from 7.4 to 6.2, providing a novel platform for translocation of tethered small molecules or nanoparticles.[1,10−12]

In our research, HAuNS were colocalized in tumor cells under pH-driven ability of pHLIP. A single light was then served as a critical factor to induce on-demand mechanisms at 3 steps (Figure 1): (1) HAuNS displayed strong photothermal coupling property under irradiation of specific light;[6] (2) Ce6 and pHLIP released from the surface of PTCAs upon heat generation;[3] (3) ROS was then generated through the reaction between Ce6 and surrounding oxygen in tissues upon the photoirradiation,[2] thus facilitating light-induced PTT-releasing-PDT step-by-step multitherapeutics.

HAuNS were synthesized by sacrificial galvanic replacement of cobalt nanoparticles based on chloroauric acid as described by Li et al.[13] Ce6 and pHLIP were then absorbed onto the surface of HAuNS to prepare HAuNS-Ce6, HAuNS-pHLIP, and HAuNS-pHLIP-Ce6, respectively. Upon the formation of HAuNS, the localized surface plasmon resonance (LSPR) peak shifted from 550 to 720 nm and broadened to cover the wavelength range of 500−800 nm (Figure 2a). It was clear that as decreasing of the concentration of chloroauric acid, there was a decline in optical density as well as a red shift. This phenomenon proved the function of various absorption cross

Received: June 29, 2015
Accepted: August 6, 2015
Published: August 6, 2015

DOI: 10.1021/acsami.5b05763
ACS Appl. Mater. Interfaces 2015, 7, 17592−17597

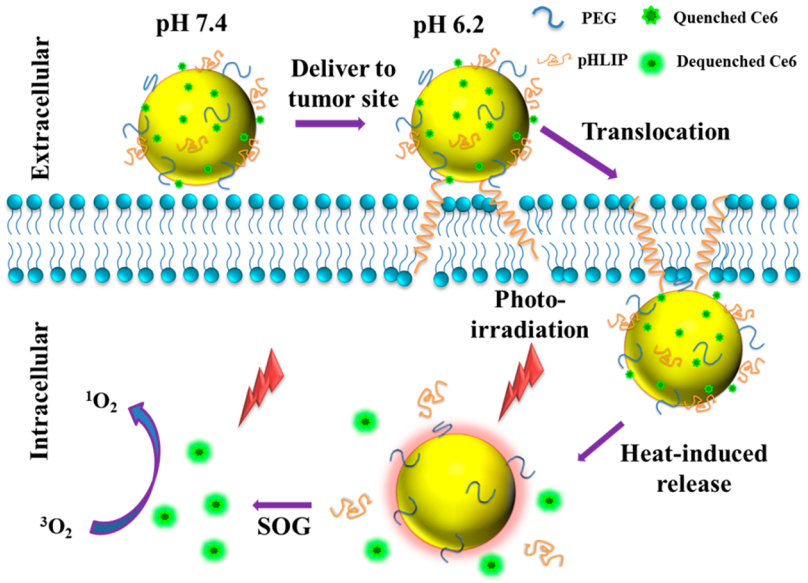

Figure 1. Schematic representation of HAuNS-pHLIP-Ce6 for PTT-releasing-PDT multitherapeutics after targeting and translocation driven by low pH value.

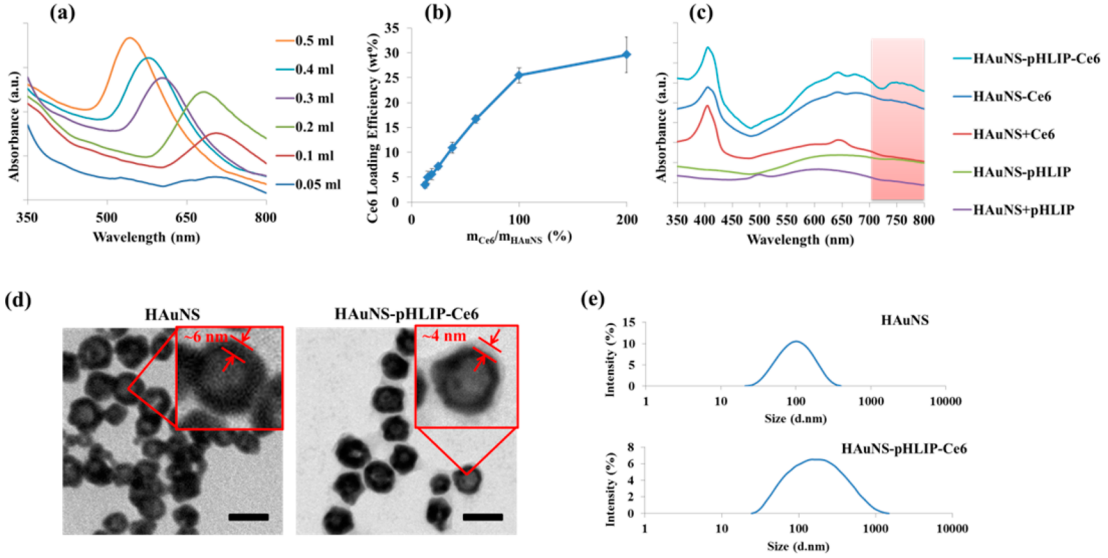

Figure 2. Formulation optimization and characterization. (a) UV−vis absorption spectra dependence on volume of added chloroauric acid (0.0025M). (b) Ce6 loading efficiency of HAuNS-pHLIP-Ce6 as a function of Ce6 concentration. (c) UV−vis spectra of simple mixtures (HAuNS +Ce6 and HAuNS+pHLIP) and formulations loading active agents by electrostatic interaction (HAuNS-Ce6 and HAuNS-pHLIP). The pink area indicated broaden absorbance range. (d) TEM images of plain and Ce6-loaded HAuNS. Scale bar indicated 50 nm. (e) Size distribution of HAuNS before and after loading active agents.

sections of the HAuNS due to the different thicknesses of gold shells. As the wall grew thicker, the absorption cross section became larger.[14] To design a PTCA in accordance with the excitation wavelength of PS, we added 0.2 mL of chlorauric acid with determined gold concentration (0.0025 M) to prepare the optimal HAuNS. Therefore, the synergistic PTT/PDT effect was facilitated by HAuNS-Ce6 complex under irradiation of 670 nm laser.

According to synthesis protocol, HAuNS were stabilized by negatively charged citrate in aqueous solution.[7] Then the positively charged HAuNS-NH_2 were obtained by functionalizing with amino groups via mercaptoethylamine. As a result, Ce6, a negative charged agent, was bound to the positive charged HAuNS-NH_2 by a charge−charge electrostatic interaction. The formation of complex between the active agents and nanocarriers was advantageous for easier fabrication and scale up as well as more predictable release compared to covalent conjugation approach. We found that the loading amount of Ce6 onto HAuNS rose linearly with the increased Ce6 concentration, and reached about 25 wt % at Ce6/HAuNS ratio of 1:1 (Figure 2b). For a comparison, the maximum loading efficiency of Ce6 onto/into the gold nanorods and gold vesicles was less than 10 and 20 wt %, respectively.[2] Further increase of Ce6 ratio, however, would not result in significantly higher loading efficiency. The exceptionally high payload of Ce6 could be explained by the greater surface area of HAuNS compared to solid gold particles. Li et al. have validated that the outer and inner surface of HAuNS could be coated with the

DOI: 10.1021/acsami.5b05763
ACS Appl. Mater. Interfaces 2015, 7, 17592−17597

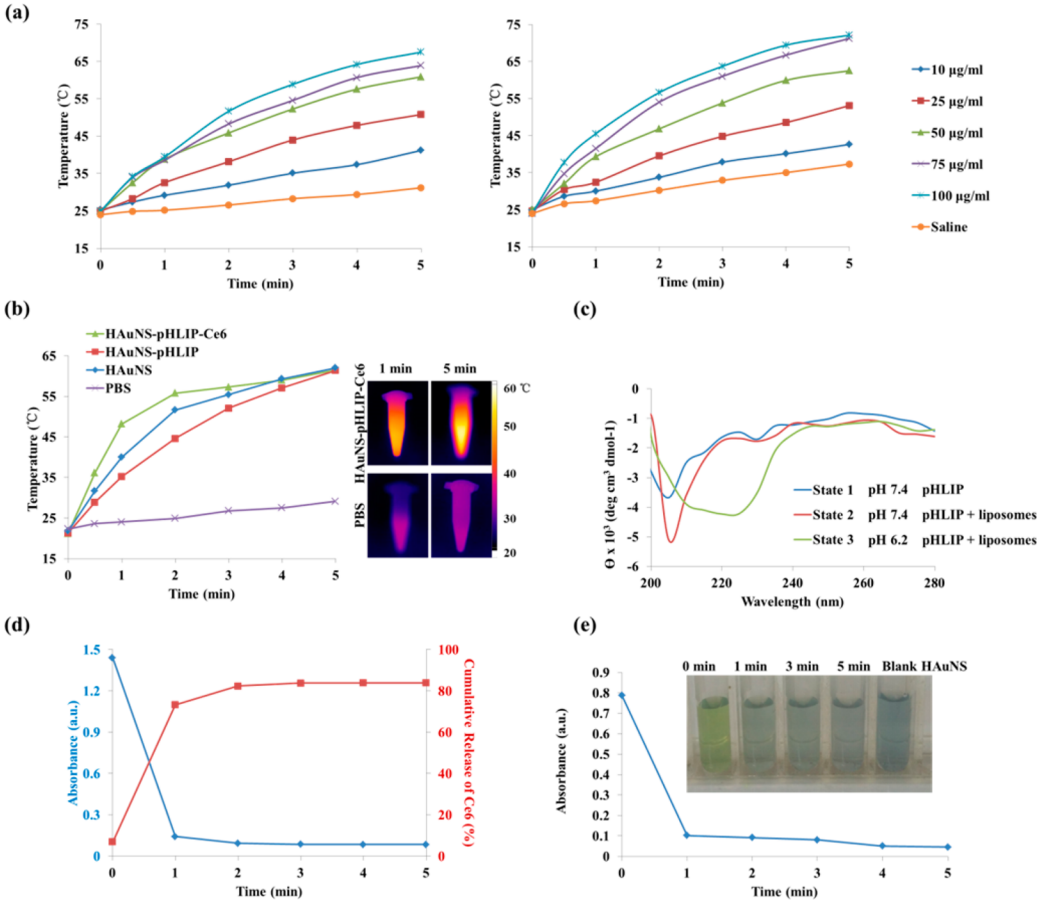

Figure 3. Photoinduced PTT-releasing-PDT multitherapeutics evaluation. (a) Temperature curves of different HAuNS concentration over a period of 5 min under exposure to light at wavelength of 670 (left) and 808 nm (right), respectively. (b) Temperature curves of different formulations over a period of 5 min under exposure to 670 nm laser irradiation. Inset: Thermographic images of various solutions at determined time intervals. (c) CD spectra of pHLIP in various solutions. (d) Time dependence release behavior and (e) SOG of HAuNS-pHLIP-Ce6 triggered by 670 nm laser. The cumulative release was determined by UV−vis absorbance of the remaining Ce6, and SOG was determined by quenched absorbance of DPBF at 410 nm. Inset: Formulation appearance as a function of laser irradiation time when mixed with DPBF or not.

contrary charged agents, and the porous gold shell made it possible for molecules to diffuse into the core and bind to the inner surface.[7]

Successful loading of Ce6 and pHLIP in HAuNS was confirmed by UV−vis absorbance curves. The absorption of HAuNS-pHLIP-Ce6 displayed the characteristic peaks of Ce6 at 410 and 650 nm. The absorption range was wider after loading of Ce6 and pHLIP through electrostatic interaction, which might be attributed to the increased thickness of gold shells (Figure 2c). Zeta potential was used to monitor the functionalization steps. The surface zeta potentials of HAuNS, HAuNS-NH_2, and HAuNS-pHLIP-Ce6 were −16.4, 18.9, and −14.3 mV, respectively. Further, the morphology of HAuNS before and after agents loading was detected by transmission electron microscopy (TEM) images (Figure 2d). The results indicated the average diameter and Au shell thickness was 40 and 6 nm, respectively. Surface modification by pHLIP and Ce6 resulted in an extra ∼4 nm thickness of the outer layer. Besides, dynamic light scattering (DLS) measurements showed the particle sizes of HAuNS and HAuNS-pHLIP-Ce6 were 86.53 nm (PDI was 0.176) and 119.2 nm (PDI was 0.192) (Figure 2e), respectively, which were much larger than observed in TEM images, might be due to the inhomogeneity and aggregation tendentiousness of gold carriers in aqueous solution.

To evaluate the 670 nm laser-induced PTT efficiency of HAuNS-pHLIP-Ce6, we exposed various samples to 808 and 670 nm laser at 2.0 W/cm^2 for 5 min (808 nm as control). Figure 3a revealed an increase in the photothermal efficacy as a function of elevation of gold concentration for HAuNS, whereas there were no significant differences in temperature change of the two wavelength laser under irradiation. Therefore, 670 nm as well as 808 nm laser could serve as good photothermal triggers to HAuNS. When exposed to 670 nm, the temperature of HAuNS solutions reached over 60 °C after 5 min, whereas saline exhibited negligible increase in temperature (Figure 3b). On the other hand, HAuNS-pHLIP-Ce6 produced a much more rapid heating effect in the first 2 min, because of the absorbance of loaded Ce6 in formulation at 670 nm.

In addition, secondary structure of pHLIP in three states was evaluated by CD spectra (Figure 3c). In this study, liposomes were used to mimic the existence of cellular membranes. pHLIP remained α-helix conformation in physiological pH conditions at state 1 and 2, while the inserted state was monitored at state 3 reflecting by changes of the CD spectral signal. The results confirmed the transmembrane ability of pHLIP in the condition of pH 6.2, which was similar to the acid microenvironment of tumor areas.

DOI: 10.1021/acsami.5b05763
ACS Appl. Mater. Interfaces 2015, 7, 17592−17597

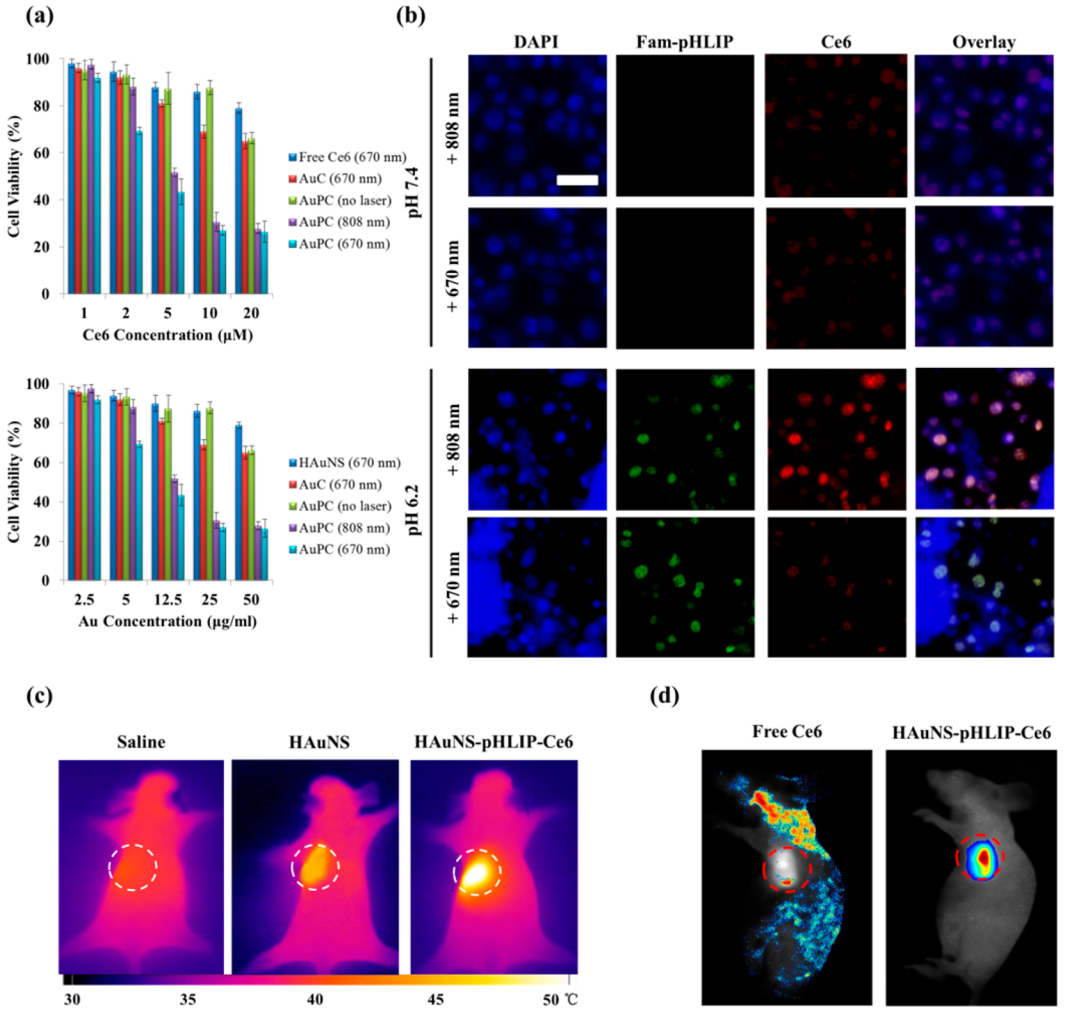

Figure 4. Evaluation of specifically therapeutics of HAuNS-pHLIP-Ce6. (a) Viability of Hela cells treated with various formulations at pH 6.2 as a function of concentrations of Ce6 (upper) and Au (lower), respectively. AuC and AuPC represented for HAuNS-Ce6 and HAuNS-pHLIP-Ce6, respectively. (b) Cellular uptake of HAuNS-pHLIP-Ce6 4 h after various treatments at pH 7.4 and pH 6.2. Scale bar indicated 25 μm. (c) Thermographic images of tumor-bearing mice after light irradiation. (d) In vivo distribution of Ce6 in nude mice bearing Hela tumors 4 h post treatment. 670 and 808 nm laser (2 W/cm^2, 5 min) were used to induce photothermal effect and Ce6 release, respectively, 12 h after i.v. administration.

Many researchers have demonstrated the phototriggered release mechanism of loaded agents from gold carriers.[3,15] First, the light could be converted to heat by gold nanocarriers. Subsequently, the electrostatic interaction between negatively charged Ce6 and positively charged carriers was evidently decreased due to the heat generation. As a result, Ce6 unloaded from the gold surface due to the decreased interaction. To investigate photoinduced in vitro release behavior of Ce6 from PTCA surface, HAuNS-pHLIP-Ce6 was irradiated upon 670 nm (2.0 W/cm^2, 5 min) laser. In the results, over 70% of Ce6 was released in the initial 1 min and followed by much lower release profile (Figure 3d). The sudden release behavior might be due to the rapid heat generated (sharply reached over 45 °C within 1 min) from the gold particles surface, thus weakening the electrostatic interaction between PS and PTCA, leading to an evidently higher release efficiency. Therefore, the 670 nm laser could perform releasing trigger as well as photothermal inducer.

To confirm the singlet oxygen generation (SOG) capability of HAuNS-pHLIP-Ce6, 1,3-diphenyl isobenzofuran (DPBF) was used as a singlet oxygen trapping reagent to quench its intrinsic absorbance via forming DPBF-endoperoxide complex after laser-irradiation.[4] As a result, the DPBF absorbance decreased dramatically under 670 nm laser, which indicated that HAuNS-pHLIP-Ce6 could efficiently generate singlet oxygen upon photoirradiation (Figure 3e).

To investigate the cytotoxicity of various formulations to Hela cells, we assessed cell viability at acid condition. Both of 808 and 670 nm lasers were used to induce PTT and synergistic PTT/PDT effect, respectively (Figure 4a). As a result, free Ce6 did not show much cytotoxicity; however, groups that combined with PTCA (HAuNS-Ce6) caused evident cell death, indicating that the PDT effect of Ce6 was depended on the generation of PTT effect due to the resonace energy transfer from PTCA to Ce6.[16] What's more, the introduction of pHLIP contributed to a greater cytotoxicity, confirming the targeting ability of pHLIP to tumor cells at low pH value.

In addition, to compare with HAuNS-pHLIP-Ce6, the formulation HAuNS-pHLIP and HAuNS-Ce6 were also incubated in cells with medium at pH 6.2 and pH 7.4 (Figure S1). The fluorescence of pHLIP and Ce6 were monitored 4 h

DOI: 10.1021/acsami.5b05763
ACS Appl. Mater. Interfaces 2015, 7, 17592−17597

after 808 nm laser-triggered release process to investigate the internalization behaviors. pHLIP signal from HAuNS-pHLIP was found in low pH value, indicating the pH driven ability of pHLIP. Ce6 signal from the formulation without pHLIP modification (HAuNS-Ce6) was found to be extremely low at both pH conditions. HAuNS-pHLIP-Ce6, however, was represented a greater internalization of Ce6 at pH 6.2. And then, the release induced by cleavage of the charge-by-charge interaction was observed in Hela cells treated with HAuNS-pHLIP-Ce6 for 4 h after photoirradiation at pH 6.2 and pH 7.4, respectively (Figure 4b). The active agents were found to be internalized evidently dependent on pH values. However, no significant signal of pHLIP or Ce6 was shown in tumor cells at pH 7.4, which indicated that pHLIP locating the outside of the cell bilayers at physiological conditions. On the contrary, tumor cells could efficiently uptake pHLIP at pH 6.2 under both lasers, suggesting the nanocarriers were colocalized with pHLIP into cells. On the other hand, both of pHLIP and Ce6 were accumulated in tumor cells under 808 nm laser due to the photoinduced release mechanism. However, significant lower Ce6 signal was found in cells after treated with 670 nm laser, which might due to the consumption of the most Ce6 by performing PDT effect after divorcing from gold surface under the multi-induce effects of this wavelength. These results demonstrated the existence of efficient pH-responsive property of pHLIP, and meanwhile confirmed the simultaneous PTT/PDT effect which induced by 670 nm laser.

Animal protocols were performed under the guidelines for humane and responsible use of animals in research set by Tianjin University. In the in vivo studies, the thermographic images indicated that HAuNS-pHLIP-Ce6 efficiently delivered PTCA to the expected areas and performed PTT effect at tumor regions of Hela tumor bearing nude mice due to the presence of pHLIP (Figure 4c). Therefore, the entire tumor volume, including the tumor/tissue interface, could be heated to over 45 °C within 5 min. In this study, Ce6 was used as an imaging agent to indicate biodistribution results (Figure 4d). What's more, 808 nm laser was utilized to dequench Ce6 fluorescence at 12 h post i.v. administration. Another 4 h later, the tumor was distinguishable from other tissues with good fluorescence contrast in the HAuNS-pHLIP-Ce6 treated group, confirming the highly specific tumor targeting effect of the tested approach due to the presence of pHLIP.

The HAuNS-pHLIP-Ce6 treated group showed remarkable delay in tumor growth compared with the other groups under irradiation of 670 nm laser after 3 weeks (Figure S2). In contrast, the HAuNS-pHLIP-Ce6 treated groups showed different tumor growth curves upon various irradiation conditions. The group without laser irradiation performed no apparent difference from control group, indicating the highly laser-dependence of the therapeutic effect. It was noteworthy that 670 nm laser treated group performed higher antitumor efficacy as compared with the group irradiated by 808 nm laser, showing the superior of the synergistic PTT/PDT effect induced by 670 nm laser. H&E stained images of tumor sections collected from saline and HAuNS-pHLIP-Ce6 groups 21 days post treatment combined with 670 nm laser (Figure S3). Histological images showed little pyknosis in saline group. On the contrary, infiltrating tumor cells with highly pleomorphic nuclei was observed in HAuNS-pHLIP-Ce6 treated group, demonstrating the effective treatment of the optimal formulation.

In summary, our studies demonstrated a novel antitumor therapeutic based on the HAuNS-pHLIP-Ce6 combined with 670 nm laser. This approach was advantageous in the following aspects: (1) HAuNS displayed relatively high loading capacity of Ce6 in terms of effective surface area; (2) the strong and broad range of absorption of HAuNS in vis-NIR region facilitated the simultaneous PTT and PDT effects at 670 nm; (3) the electrostatic interaction between the active agents and the PTCA surface could be decreased under PTT effect, thus leading to a photoinduced release; (4) the presence of active targeting probe pHLIP facilitated nanocarriers to colocalize in tumor cells to perform specific therapeutic effects. This novel treatment system was a promising approach to antitumor therapy based on the single light-induced PTT-releasing-PDT step-by-step therapeutic mechanism.

■ ASSOCIATED CONTENT

Supporting Information

The Supporting Information is available free of charge on the ACS Publications website at DOI: 10.1021/acsami.5b05763.

Experimental section and additional figures (PDF)

■ AUTHOR INFORMATION

Corresponding Authors

*E-mail: tanfengping@163.com. Tel.: +86-022-27405160.

* E-mail: linan19850115@163.com. Tel.: +86-022-27404986.

Notes

The authors declare no competing financial interest.

■ ACKNOWLEDGMENTS

We acknowledge the financial supports by Tianjin Research Program of Application Foundation and Advanced Technology (15JCQNJC13800) and National Basic Research Project (2014CB932200) of the MOST. We also acknowledge the support by Dr. Jun Dai for providing of Hela cell line.

■ REFERENCES

(1) Wang, N. N.; Zhao, Z. L.; Lv, Y. F.; Fan, H. H.; Bai, H. R.; Meng, H. M.; Long, Y. Q.; Fu, T.; Zhang, X. B.; Tan, W. H. Gold Nanorod-Photosensitizer Conjugate with Extracellular pH-Driven Tumor Targeting Ability for Photothermal/Photodynamic Therapy. *Nano Res.* **2014**, *7*, 1291−1301.

(2) Lin, J.; Wang, S. J.; Huang, P.; Wang, Z.; Chen, S. H.; Niu, G.; Li, W. W.; He, J.; Cui, D. X.; Lu, G. M.; Chen, X. Y.; Nie, Z. H. Photosensitizer-Loaded Gold Vesicles with Strong Plasmonic Coupling Effect for Imaging-Guided Photothermal/Photodynamic Therapy. *ACS Nano* **2013**, *7*, 5320−5329.

(3) Jang, B.; Park, J. Y.; Tung, C. H.; Kim, I. H.; Choi, Y. Gold Nanorod-Photosensitizer Complex for Near-Infrared Fluorescence Imaging and Photodynamic/Photothermal Therapy *In Vivo*. *ACS Nano* **2011**, *5*, 1086−1094.

(4) Gollavelli, G.; Ling, Y. C. Magnetic and Fluorescent Graphene for Dual Modal Imaging and Single Light Induced Photothermal and Photodynamic Therapy of Cancer Cells. *Biomaterials* **2014**, *35*, 4499−4507.

(5) Tian, B.; Wang, C.; Zhang, S.; Feng, L.; Liu, Z. Photothermally Enhanced Photodynamic Therapy Delivered by Nano Graphene Oxide. *ACS Nano* **2011**, *5*, 7000−7009.

(6) You, J.; Zhang, R.; Xiong, C. Y.; Zhong, M.; Melancon, M.; Gupta, S.; Nick, A. M.; Sood, A. K.; Li, C. Effective Photothermal Chemotherapy Using Doxorubicin-Loaded Gold Nanospheres That Target EphB4 Receptors in Tumors. *Cancer Res.* **2012**, *72*, 4777−4786.

DOI: 10.1021/acsami.5b05763
ACS Appl. Mater. Interfaces 2015, 7, 17592−17597

(7) You, J.; Zhang, G. D.; Li, C. Exceptionally High Payload of Doxorubicin in Hollow Gold Nanospheres for Near-Infrared Light-Triggered Drug Release. *ACS Nano* **2010**, *4*, 1033−1041.
(8) Dougherty, T. J.; Gomer, C. J.; Henderson, B. W.; Jori, G.; Kessel, D.; Korbelik, M.; Moan, J.; Peng, Q. Photodynamic Therapy. *J. Natl. Cancer Inst.* **1998**, *90*, 889−905.
(9) Weerakkody, D.; Moshnikova, A.; Thakur, M. S.; Moshnikova, V.; Daniels, J.; Engelman, D. M.; Andreev, O. A.; Reshetnyak, Y. K. Family of pH (Low) Insertion Peptides for Tumor Targeting. *Proc. Natl. Acad. Sci. U. S. A.* **2013**, *110*, 5834−5839.
(10) Yao, L.; Daniels, J.; Moshnikova, A.; Kuznetsov, S.; Ahmed, A.; Engelman, D. M.; Reshetnyak, Y. K.; Andreev, O. A. pHLIP Peptide Targets Nanogold Particles to Tumors. *Proc. Natl. Acad. Sci. U. S. A.* **2013**, *110*, 465−470.
(11) Zhao, Z. L.; Meng, H. M.; Wang, N. N.; Donovan, M. J.; Fu, T.; You, M. X.; Chen, Z.; Zhang, X. B.; Tan, W. H. A Controlled-Release Nanocarrier with Extracellular pH Value Driven Tumor Targeting and Translocation for Drug Delivery. *Angew. Chem., Int. Ed.* **2013**, *52*, 7487−7491.
(12) Cheng, C. J.; Bahal, R. B.; Babar, I. A.; Pincus, Z.; Barrera, F.; Liu, C.; Svoronos, A.; Braddock, D. T.; Glazer, P. M.; Engelman, D. M.; Saltzman, W. M.; Slack, F. J. MicroRNA silencing for cancer therapy targeted to the tumour microenvironment. *Nature* **2014**, *518*, 107−110.
(13) Lu, W.; Xiong, C.; Zhang, G.; Huang, Q.; Zhang, R.; Zhang, J. Z.; Li, C. Targeted Photothermal Ablation of Murine Melanomas with Melanocyte-Stimulating Hormone Analog-Conjugated Hollow Gold Nanospheres. *Clin. Cancer Res.* **2009**, *15*, 876−886.
(14) Schwartzberg, A. M.; Olson, T. Y.; Talley, C. E.; Zhang, J. Z. Synthesis, Characterization, and Tunable Optical Properties of Hollow Gold Nanospheres. *J. Phys. Chem. B* **2006**, *110*, 19935−19944.
(15) Kuo, T. R.; Hovhannisyan, V. A.; Chao, Y. C.; Chao, S. L.; Chiang, S. J.; Lin, S. J.; Dong, C. Y.; Chen, C. C. Multiple Release Kinetics of Targeted Drug from Gold Nanorod Embedded Polyelectrolyte Conjugates Induced by Near-Infrared Laser Irradiation. *J. Am. Chem. Soc.* **2010**, *132*, 14163−14171.
(16) Wang, X.; Liu, K.; Yang, G. B.; Cheng, L.; He, L.; Liu, Y. M.; Li, Y. G.; Guo, L.; Liu, Z. Near-Infrared Light Triggered Photodynamic Therapy in Combination with Gene Therapy Using Upconversion Nanoparticles for Effective Cancer Cell Killing. *Nanoscale* **2014**, *6*, 9198−9205.

DOI: 10.1021/acsami.5b05763
ACS Appl. Mater. Interfaces 2015, 7, 17592−17597